Summer 2023

Scalable and Continuous Fabrication of Dendrimer based Gene and Protein Delivery Systems

Joseph Johnston
Missouri University of Science and Technology

Recommended Citation

SCALABLE AND CONTINUOUS FABRICATION OF DENDRIMER BASED GENE

AND PROTEIN DELIVERY SYSTEMS

by

JOSEPH TIMOTHY JOHNSTON

A THESIS

Presented to the Graduate Faculty of the

MISSOURI UNIVERSITY OF SCIENCE AND TECHNOLOGY

In Partial Fulfillment of the Requirements for the Degree

MASTER OF SCIENCE IN CHEMICAL ENGINEERING

2022

Approved by:

Dr. Hu Yang, Advisor
Dr. Jee-Ching Wang
Dr. Anthony Convertine

ABSTRACT

Gene and protein therapeutics play critical roles in the drug market and represent the future of biopharmaceuticals. Polymeric nanoparticle-based gene/protein delivery systems are promising owing to their ability to protect the cargo from degradation, improving intracellular delivery and transfection efficiency as well as abundant sources and flexibility to be modified. Yet the successful industrialized production and clinical application of polymeric nanoparticle-based delivery systems have long been limited by unsatisfied delivery efficiency and the lack of reproducible and scalable methods for the preparation of uniform nanoparticles with good batch to batch consistency. To address the unsatisfied efficacy and difficulty in scale-up preparation of traditional gene and protein delivery systems, the goal of this project is to validate a scalable and reproducible fabrication technology that uses a water-based continuous nanoparticle generation platform (wNGP) for scalable production of uniform and highly efficient gene and protein delivery systems using functionalized polyamidoamine (PAMAM) dendrimers. The generation platform is a multi-inlet vortex mixer that was originally designed for flash nanoprecipitation. The feasibility of the application of this technology in the biopharmaceutical industry will be verified by the fabrication of a polymer/plasmid and polymer/protein nanocomplex using a functionalized PAMAM dendrimer and a model plasmid and protein. Key process parameters were identified to fabricate the nanocomplexes in a scalable way without sacrificing functionality.

ACKNOWLEDGMENTS

I would like to acknowledge and show my appreciation to my thesis advisor, Dr. Hu Yang for graciously accepting me into his group, and consistently encouraging and supporting me throughout my research. He always believed in me and taught me the skills for me to succeed as a graduate student. I am very fortunate to have worked under his expert guidance. I would also like to thank Dr. Jee-Ching Wang, and Dr. Anthony Convertine for serving as my committee members.

Secondly, I would like to thank the Missouri S&T Chemical Engineering Department for providing me academic support through a graduate teaching assistantship in the Unit Operations Laboratory. I thoroughly enjoyed working with Dr. Christi Luks, Matthew Senter, and Micheal Murphy. I would also like to extend a great appreciation to Dr. Da Huang, Dr. Jawahar Khetan, Vidit Singh, and Anna Chernatynskaya for offering me continuous moral support, and becoming some of my closest friends during my time as a graduate student. It would have been difficult to complete this project without their knowledge and support.

Finally, I would like to express my greatest appreciation to my parents Tim and Marty, and my sisters Jenny and Kristin. They have always been my biggest supporters, and the greatest role models in teaching me how to succeed across all walks of life. Their motivation, encouragement, and love has been the largest driving force behind this achievement.

TABLE OF CONTENTS

Page

LIST OF ILLUSTRATIONS

LIST OF TABLES

NOMENCLATURE

Symbol	Description
μ	Dynamic Viscosity
ρ	Fluid Density
ν	Fluid velocity
D	Diameter

1. INTRODUCTION

1.1 GENES AND PROTEINS AS THERAPEUTICS

Gene therapies and protein therapeutics are the most promising options for treating a wide range of diseases such as cancer, cardiovascular disease, and immunodeficiency. They play critical roles in the drug market and represent the future of biopharmaceuticals. The concept of gene therapy is to introduce a piece of genetic material into target cells that will result in either a cure for the disease or a slowdown in the progression of the disease (Verma & Weitzman, 2005). This can be done by replacing a disease-causing gene with a healthier copy, or by inactivating a gene that is known to cause diseases or is not functioning properly. Typical gene therapy products include plasmid DNA, mRNA, and patient-derived genes. Proteins have the most dynamic and diverse role of any macromolecule in the body (Leader, Baca, & Golan, 2008), and have many different functionalities such as forming channels in membranes, providing cellular support, and catalyzing reactions. The wide functionality of proteins allows for more advantages over drugs as a therapeutic agent since they are highly specific in how they interact with biological processes. This can lead to a decreased chance of protein-based therapeutics to stimulate an immune response since many proteins are produced by the body naturally. The most common example of protein based therapeutics is for the treatment of Type I Diabetes, using recombinant insulin as a protein therapeutic (Banting, Best, Collip, Campbell, & Fletcher, 1922). One of the largest challenges employing genes and proteins as therapeutics is by having a delivery system that can deliver these components into target cells. To overcome this barrier, it is required to encapsulate these

therapeutic agents into a delivery system that can successfully transfer their payload into cells.

1.2. DRUG DELIVERY SYSTEMS

Currently, viral-based gene transfection platforms account for the majority of vehicles used in gene therapy clinical trials. However, safety concerns motivate the need to engineer alternate gene transfection platforms. Nonviral gene delivery systems, including liposomes, polymeric nanoparticles, dendrimers, inorganic nanoparticles, and so on, have been developed to address the primary limitations associated with viruses, such as the potential for immune responses, insertional mutagenesis, and issues with large-scale production. Similar to gene therapy, protein therapeutics suffer from the limitations of poor stability, low cell membrane permeability, immunogenicity, and short half-life, but they are one of the fastest-growing classes of drugs on the market. Nonviral nanoparticle technology provide advantages as a drug delivery system due to their specific properties. These advantages include improved bioavailability, increased half-life/decreased clearance from the body, and targeting to a specific location within the body which can lead to lower dosing and enhanced therapeutic effect as compared to free drugs (Mudshinge, Deore, Patil, & Bhalgat, 2011).

1.3. DENDRIMERS FOR DRUG DELIVERY

Dendrimers are a polymer-based nanostructure with a symmetrical branched structure, and a high density of functional end groups (Mudshinge et al., 2011). Their highly clustered surface groups allow for a wide range of conjugation giving them a

multitude of biomedical applications such as: targeted drug delivery, gene and protein

delivery, bioimaging, and small molecule drug payloads to enhance therapeutic

effectiveness. Polyamidoamine (PAMAM) dendrimers, shown in Figure 1.1., have

primary amino groups on their surface that can interact with nucleic acids and condense

them into more stable and protected particles.
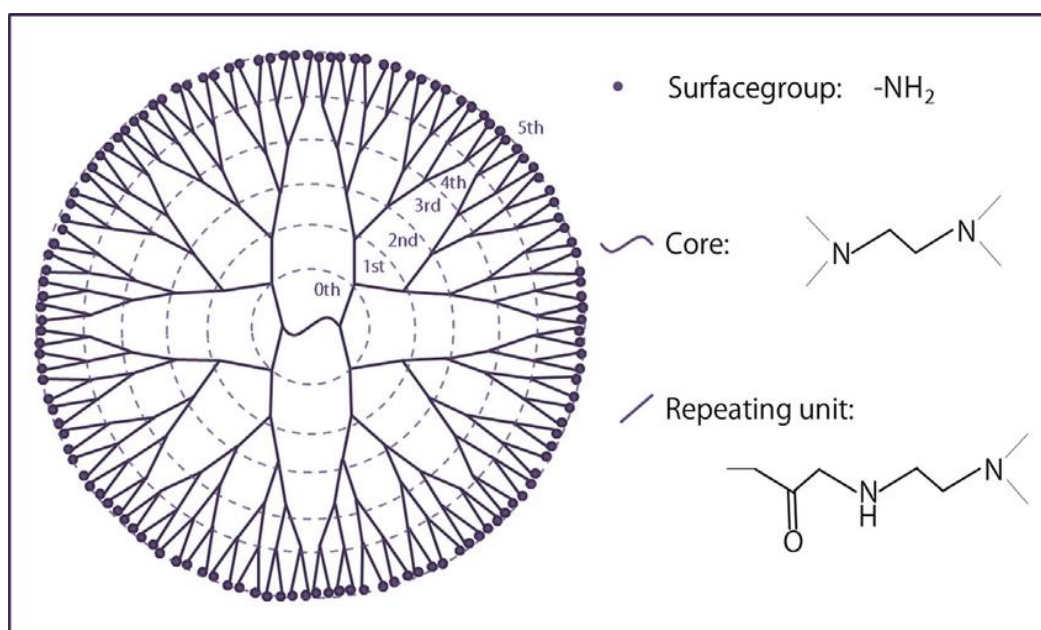
Figure 1.1. PAMAM Dendrimer Structure (Berényi, Mihaly, Wacha, Toke, & Bóta, 2014)

PAMAM dendrimers also help facilitate cellular internalization through

endocytosis. However, one of the issues with higher generation dendrimers is that they

pose significant toxicity to cells. To combat toxicity, a successfully proven approach is to

conjugate polyethylene glycol (PEG) to the surface of the dendrimer, which also

enhances its solubility. PEGylated dendrimers are favored for biological applications

since they can enhance structural stability of DNA loaded complexes (Yuan, Yeudall, &

Yang, 2010). In the case of protein therapy, dendrimer protein conjugation can

successfully be completed by surface enhancement such that the dendrimer can conjugate

with both cationic and anionic groups on the protein surface. Phenylboronic acid (PBA)

is an electron-deficient group that can coordinate with cationic amine and imidazole

groups on proteins via nitrogen-boronate complexation (C. Liu et al., 2019). In

conjunction, amine groups on the dendrimer can conjugate with anionic species on the

protein surface. Figure 1.2. below highlights fundamentals of dendrimers for drug
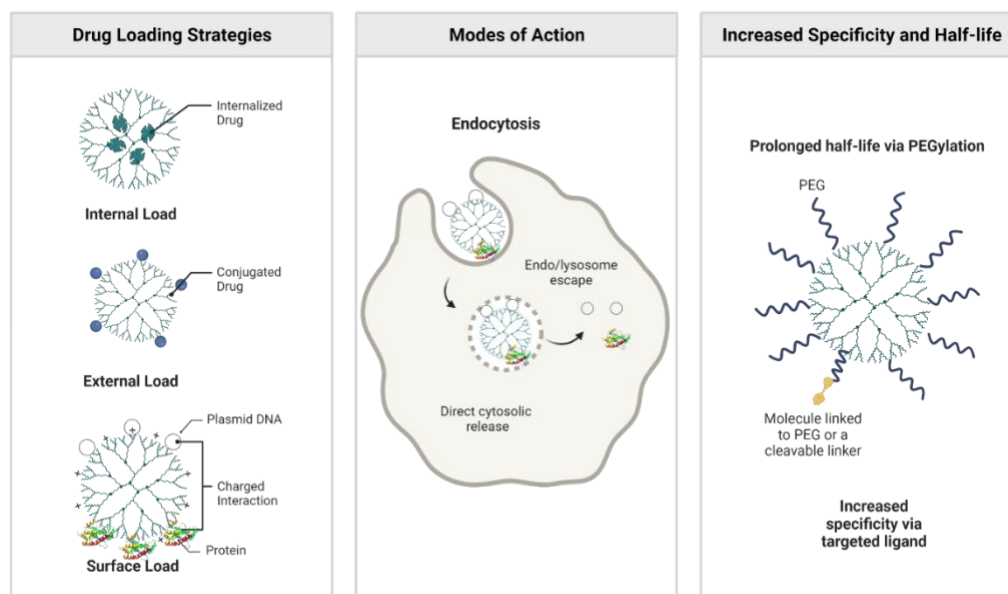
delivery.

Figure 1.2. Dendrimer Based Drug Delivery Fundamentals

1.4. BATCH AND CONTINUOUS SYNTHESIS METHODS

Nanocomplexes are formed through charge interactions between polymers and DNA/protein that results in a nanocomplex where the payload is either encapsulated or conjugated on the surface. Dendrimer based gene and protein nanocomplexes are traditionally made in a simple batch mixing process. Each component is dissolved in a solution, then combined at the desired weight ratios and vortexed thoroughly, then incubated before use as shown in Figure 1.3. below. These are traditionally made in small volumes in the range of 1-5 mL and made on an as needed basis.
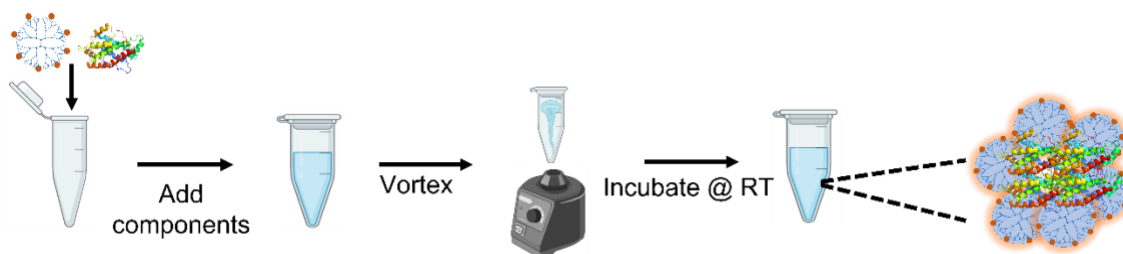
Figure 1.3. Lab Scale Batch Process for Nanocomplex Generation

A major setback from the batch process is the difficulty to scale-up. Vortex mixing is a random process that is difficult to replicate the same mixing conditions to produce consistent nanocomplex size distributions and may result in poor stability of produced nanocomplexes. The randomness in the mixing poses a significant hinderance to scaling up the mixing process for large scale production. Successful industrialized production and clinical application of polymeric nanoparticle-based delivery systems

have been limited by the lack of scalable methods for preparation of uniform

nanoparticles with good batch to batch consistency. Rapid mixing processes have been

developed through a method known as flash nanoprecipitation. Flash nanoprecipitation

(FNP) shows advantages of fast processing, simple equipment, and narrower size

distributions of nanoparticles produced (Zhu, 2014). This process involves dissolving a

hydrophobic drug and a polymer in an organic solvent that is miscible with water. The

organic solution is injected into a small chamber with water at a high velocity to force the

drug and polymer to precipitate and rapidly form nanoparticles. This process was first

developed using a confined impinging jet mixer (CIJ) (Johnson & Prud'homme, 2003).

In this design, two streams are fed into a confined mixing chamber at high

velocity to induce turbulence. This mixer design serves as a continuous platform that

allows for continuous feeding of raw material solutions and collection of the formed

product. A drawback to this design is that both inlet streams must operate at equal

momentum to prevent backflow and maximize turbulence in the mixer. To overcome this

limitation, researchers developed a Multi-Inlet Vortex Mixer (MIVM). Similar to the CIJ

mixer, the MIVM operates such that each stream contributes independently to drive

micro mixing in the chamber (Y. Liu, Cheng, Liu, Prud'homme, & Fox, 2008). In this

design it is possible to operate streams at different flow rates or introduce more

components into the mixing chamber. A schematic for both the confined impinging jet

mixer, and the MIVM and how they can be used for nanocomplex manufacturing is

shown below in Figure 1.4.
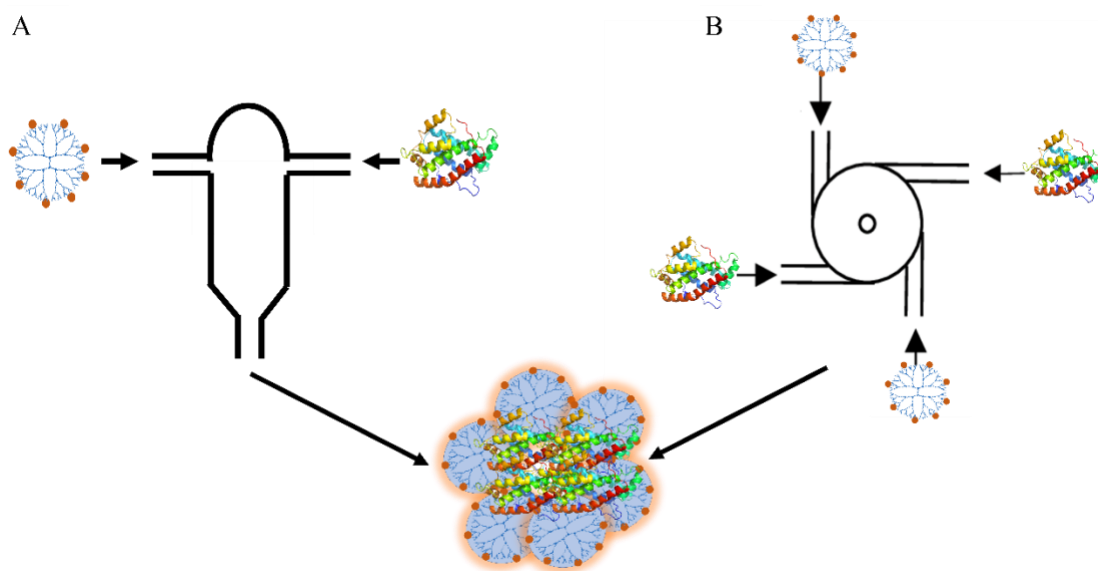
Figure 1.4. Mixing devices for Continuous Manufacturing of Nanocomplexes (A) Confined Impinging Jet Mixer and (B) Multi-Inlet Vortex Mixer

Although originally designed for flash nanoprecipitation, these designs can be used as a continuous platform for rapid mixing of components. The mixing regime is determined by the combined momentum of each stream to induce turbulence which can be characterized by calculating the Reynolds number. The overall Reynolds number of the system acts as a design parameter in scaling up the size of the mixer to allow for larger volumetric flow rates, which in turn leads to large scale production of nanoparticles. In conjunction with Reynolds number, the residence time the material spends in the mixer is another important parameter used for scaling.

2. EXPERIMENTATION

2.1. DENDRIMER PREPARATION AND CONJUGATION

Two dendrimer formulations were synthesized for use in nanocomplex formulations using a fifth generation (G5) diaminobutane core polyamidoamine (PAMAM) dendrimer, G5-PEG(polyethylene glycol) and G5-PBA(phenylboronic acid). Both reaction schemes are shown below in Figure 2.1. G5-PEG(3.4k) was synthesized through a one-step reaction between G5 and PEG-NHS ester at a 15:1 molar ratio in 0.1M sodium bicarbonate buffer. The basic condition allows the amine groups on G5 to remain in a molecular form which has high affinity for the NHS ester. The reaction efficiency was evaluated in a small batch scale using 50 mg of G5 dissolved in 15 mL of sodium bicarbonate. PEG-NHS was dissolved in separate buffer then quickly added to the G5 solution and allowed to react for 24 hours at room temperature under heavy agitation. The solution was then transferred to a 3.5k dialysis membrane and run against RO water to remove any unreacted components. Dialysis water was changed every 12 hours at least 3 times to ensure complete removal of unreacted components. The solution was then transferred to a pre-weighed 50 mL tube and frozen at -80 °C for 24 hours, or flash frozen in liquid nitrogen until it was completely frozen. This frozen solution was then lyophilized at 0 mBar and -50 °C for 2-3 days, or until all water was removed and the dried powder was stored at -20 °C. When ready to use, the dried powder was weighed and dissolved in water or PBS at appropriate stock concentrations.
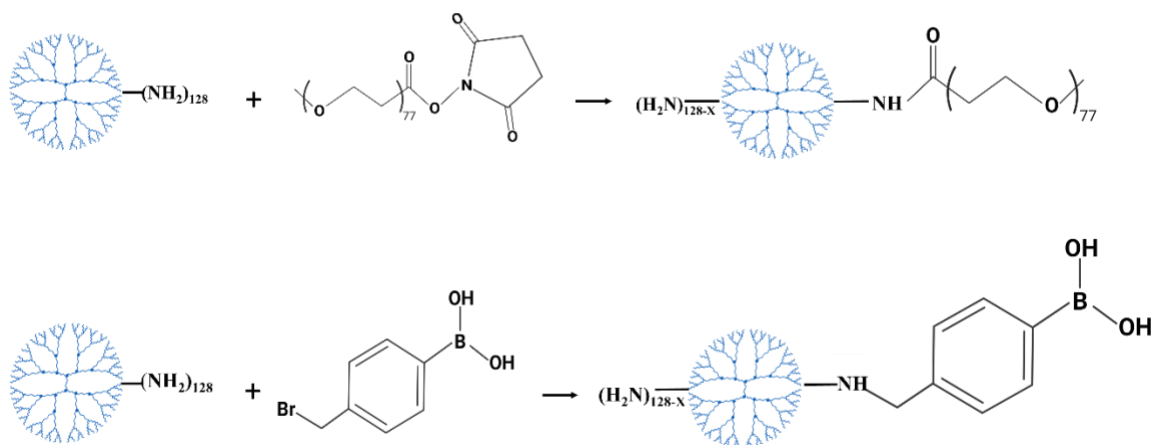
Figure 2.1. PAMAM G5 Dendrimer Conjugation Reactions

G5-PBA was synthesized by reacting G5 with 4-bromomethylphenylboronic acid

in a one-step reaction to couple PBA to the amine groups on G5 dendrimer. PBA was

dissolved with G5 in anhydrous methanol at a 66:1 molar ratio (PBA:G5) and allowed to

react for 24 hours at room temperature under heavy agitation. Similar to the G5-PEG

formulation, the solution was dialyzed to remove unreacted components. In this

formulation the first dialysis was run against methanol to enhance the removal of

unconjugated PBA. Subsequent dialysis was thoroughly run against RO water to allow

for complete solvent exchange with methanol. The solution was frozen at -80 C, and

lyophilized at the same conditions mentioned above, and the obtained powder was stored

in a desiccator.

Both formulations were measured through HNMR spectroscopy to determine the

degree of conjugation using D_2O as the solvent. Once the reaction conditions were

optimized to yield the desired conjugation level for each formulation, the synthesis was scaled-up to produce larger batches. Each batch was measured by HNMR to confirm its conjugation before use in nanocomplex formulations.

2.2. PLASMID DNA PRODUCTION AND PROTEIN PREPARATION

A green fluorescent protein encoding plasmid pcDNA3-EGFP was a gift from Doug Golenbock (Addgene plasmid # 13031 ; http://n2t.net/addgene:13031 ; RRID:Addgene_13031) was used as a model plasmid for DNA complexation. Due to the large amount of DNA needed for scale-up continuous manufacturing experiments, the plasmid was transformed in DH5α *Escherichia coli* and grown to replicate the plasmid, then purified from the bacteria. Transformed bacteria containing pcDNA3-EGFP was streaked in agar plates to isolate the cells containing the plasmid, then inoculated in growth media to replicate plasmid containing bacterial cells. As depicted in Figure 2.2. below, agar plates were made by mixing Luria Broth Agar with purified RO water according to the manufacturer's instructions in 100 mL batches, then autoclaved for 15 mins at 121 ℃ and 15 psig. After autoclave cycle was complete the flask was placed in a 55 ℃ water bath to cool down the solution to prevent thermal degradation of the antibiotic. pcDNA3-EGFP contains an ampicillin resistant gene which protects the bacterial cells from antibiotic treatment in order to isolate cells that contain this plasmid. Ampicillin was added to the agar at a concentration of 100 µg/mL and mixed thoroughly, then the solution was poured into petri dishes and allowed to harden.

1. Sterilized Agar solution
2. Pour liquid nutrient agar
3. Streak plate with Bacteria
4. Incubate at 37 °C for 24 hours
5. Colonies grow on plate
6. Inoculate Bacteria in growth media
7. Shake at 120 rpm in 37 °C for 8-10 hours
8. Separate Bacteria into flasks and centrifuge
9. Discard supernatant, store pellet at -80 °C
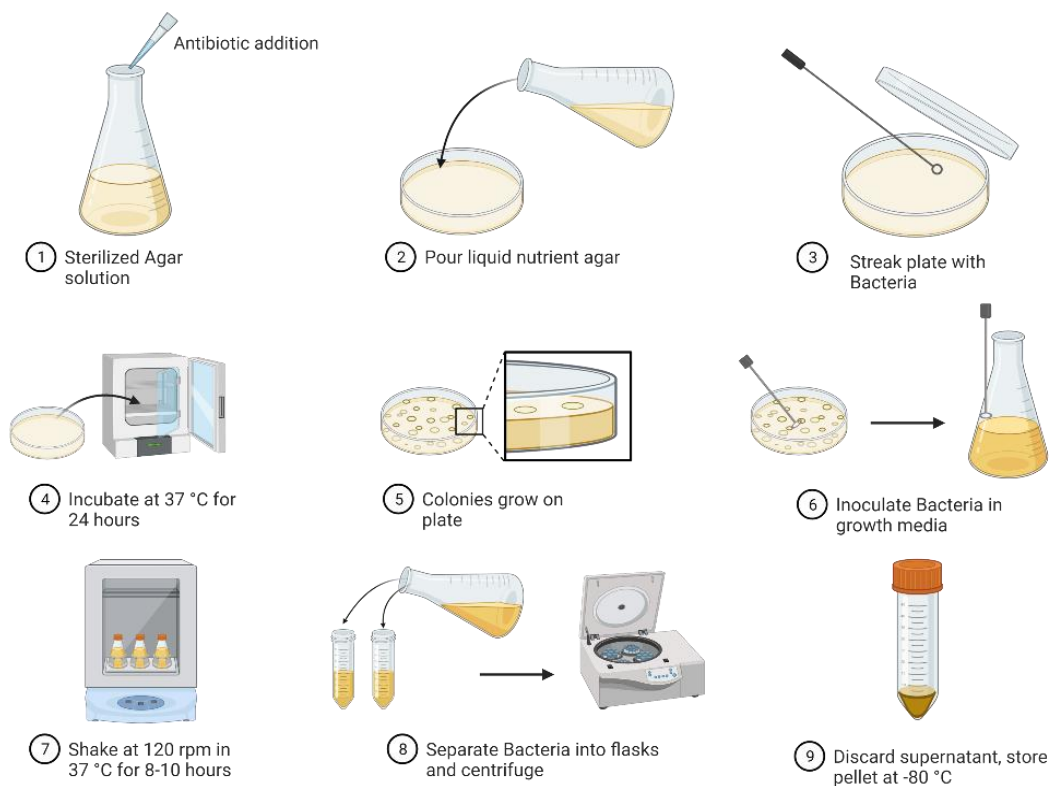
Figure 2.2. Bacterial Cell Culture Growth Schematic

Once the agar plates were hardened, the transformed bacteria stock was streaked onto the plate using a sterile loop and the plates were covered and incubated in a 37 ℃ oven in high humidity for 24 hours. Once visible bacterial colonies were on the plates, the growth was halted by placing the plates in a 4 C refrigerator. Single isolated colonies were chosen from the agar plates for inoculation since these are known to contain the plasmid of interest due to growth on the antibiotic containing agar plate. 2xYT media was used for inoculation and prepared in 250 mL batches. The media recipe used was 16 g/L Tryptone, 10 g/L Yeast Extract, and 5 g/L Sodium chloride. For optimal growth

conditions, the media was split between 500 mL Erlenmeyer tall neck flasks in 125 mL

aliquots to allow for adequate aeration when placed in a shaker incubator. These flasks

were autoclaved, then after allowed to cool to room temperature, ampicillin was added at

100 µg/mL to each flask to ensure only plasmid containing bacterial cells would grow.

The flasks were inoculated with single colonies from agar plates using a sterile loop and

placed in a shaker incubator for 8-10 hours at 37 °C and 120 rpm. The flasks were placed

on ice to halt growth and aliquoted into 50 mL tubes, then centrifuged at 9000 rpm for 10

minutes. The supernatant was discarded, and the bacteria pellet was stored at -80 °C until

ready for use. The plasmid was purified using ThermoFisher Scientific GeneJet Miniprep

Kit, or by a scaled-up alkaline lysis procedure.

Bovine Serum Albumin (BSA) was purchased from Sigma-Aldrich as a

lyophilized powder that was used for protein complexation. Stock solutions of BSA were

made in sterilized tubes with purified RO water and stored at -20 °C. Fresh protein stocks

were made frequently to prevent degradation.

2.3. MULTI-INLET VORTEX MIXER DESIGN AND FLUID DYNAMICS

A multi-inlet vortex mixer (MIVM) was 3D printed by stereolithography process

in a Form labs Form 3L printer. The MIVM was printed using Form labs clear resin to

allow for optical transparency to monitor and confirm fluid flow at varying flow rates.

After printing, the mold was sonicated in a bath of 91% isopropanol for 15 minutes to

remove any excess resin. The MIVM structure was then cured at 60 °C under a 405 nm

UV light for 15 minutes with constant rotation. The 3D product can be seen below in

Figure 2.3. with a clear image of the geometry, as well as ability to monitor flow regimes inside the mixer.
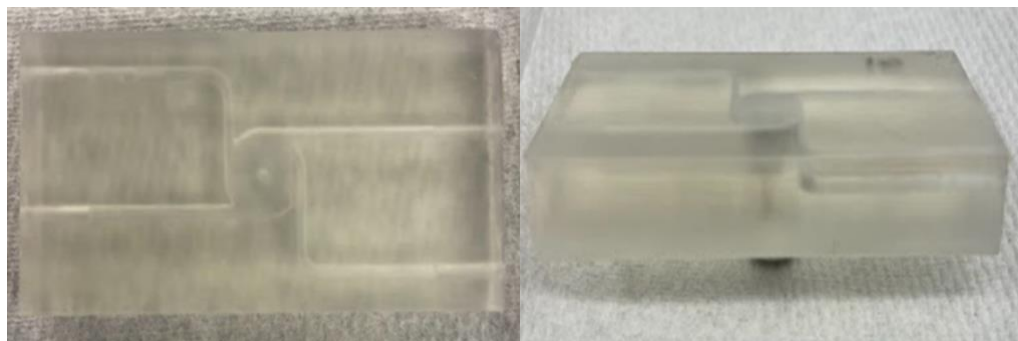
Figure 2.3. 3D Printed Multi-Inlet Vortex Mixer

The MIVM was operated by loading 4, 50 mL syringes that were connected to the MIVM through luer lock fittings and tygon tubing. Two syringe pumps were used to feed the material into the MIVM, and the outlet was collected in a small flask. Fluid dynamic testing was done in the MIVM using purified water fed by varying pump flow rates. The inlet and outlet flowrates were measured to determine Reynolds number and residence time in the mixing chamber. The MIVM was thoroughly washed with purified RO water after each use and dried with compressed air to prevent contamination between different batches. Before each use, the MIVM was flushed with the desired solvent used to prepare the feeding tubes and mixer for fluid flow by reducing friction in the tubing and channels. The first 1-2 mL of product collected from the MIVM is discarded since this primarily contains liquid from the prewashing step.

2.4. NANOCOMPLEX GENERATION

Nanocomplex production was carried out on both a batch and continuous mixing process to compare the quality and uniformity across both platforms. Nanocomplexes were produced in a batch mixing process to determine optimal weight ratio parameters, and as a comparison against those produced by the continuous method. Plasmid DNA was complexed with G5-PEG(3.4k) at various weight ratios (10:1, 15:1, 20:1, 25:1, 30:1 G5-PEG:DNA) with a plasmid loading concentration of 10 µg/mL. BSA was complexed with G5-PBA at a 1.33:1 weight ratio (BSA:G5-PBA) with a BSA loading concentration of 200 µg/mL . Batch production was done by mixing equal volumes of G5 dendrimer and either plasmid DNA or protein, and then vortexed for 15-30 seconds. Dendrimers and DNA/Protein were dissolved in purified RO water or PBS 1X at their appropriate concentrations. Nanocomplexes were produced in a continuous mixing process utilizing the MIVM. The same formulations were produced as mentioned in the batch process at the optimized weight ratios. Dendrimer solutions were fed into two opposing inlets, and DNA/Protein solutions were fed into the remaining inlets. As depicted in the figure below, each component was fed in an alternating pattern to encourage component contact in the mixing chamber and fed at the same flow rate to maximize mixing and prevent potential backflow into one of the inlet streams. Both formulations were tested at various volumetric flow rates (10-50 mL/min) to evaluate the effect of different mixing regimes on nanocomplex formation. A schematic of the continuous setup is shown below in Figure 2.4.
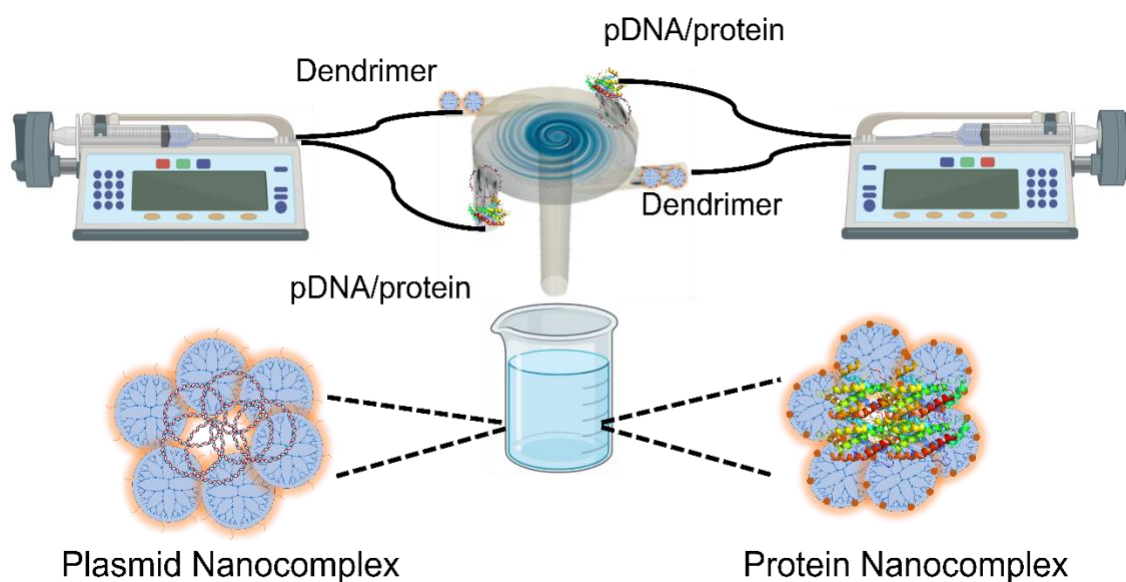
Figure 2.4. Schematic of Setup for Continuous Production of Nanocomplexes

2.5. NANOCOMPLEX FORMATION VERIFICATION

Plasmid DNA nanocomplex formation and weight ratio optimization was

evaluated through gel electrophoresis on a 0.8% agarose gel with ethidium bromide

staining. Three plasmid controls were used at decreasing concentrations to approximate

the amount of free plasmid from the nanocomplexes by comparing the intensity of the

bands. BSA protein nanocomplex formation was verified through Fluorescence

Resonance Energy Transfer (FRET) assay. To perform FRET assay G5-PBA was tagged

with Rhodamine B Isothiocyanate (RBITC) by reacting at a 5:1 molar ratio (RBITC:G5-

PBA) in anhydrous methanol for 24 hours and purified through the same dialysis

procedure mentioned previously. BSA was tagged with Fluorescein Isothiocyanate

(FITC) which was purchased from Sigma-Aldrich at a conjugated ratio of 5:1

(FITC:BSA). Fluorescently labeled dendrimer and protein were mixed and incubated for

30 minutes then measured using a Spectrofluorometer with excitation and emission

wavelengths of 470 and 500-700 nm respectively. Size distribution and zeta potential of nanocomplexes produced by batch and continuous methods were measured by dynamic light scattering on a Malvern Zetasizer. Short-term stability of both DNA and Protein nanocomplexes were briefly investigated by monitoring size distribution over time.

2.6. CYTOTOXICITY OF NANOCOMPLEXES

Cytotoxicity was carried out to determine the toxicity of the dendrimer formulations in mammalian cells. Toxicity was evaluated in NIH3T3 mouse embryonic fibroblast cells using a CCK8 assay. Since toxicity of the nanocomplexes comes from the dendrimer and not DNA/Protein, only the dendrimer was tested to determine toxicity limits for treatment. NIH3T3 cells were seeded in a 96 well plate at a density of 10,000 cells/well and allowed to incubate at 37 ℃ overnight in supplemented Dulbecco's Modified Eagle Medium (DMEM). Once the cells were attached, the medium was replaced and the dendrimer solutions were added at concentrations of 20, 40, 80 and 100 µg/mL and allowed to incubate for 24 hours at 37 ℃. After incubation, media was replaced and CCK8 reagent was added and incubated for 4 hours at 37 ℃, then absorbance at 450 nm was measured using a microplate reader.

2.7. TRANSFECTION EXPERIMENTS

Gene transfection was evaluated in NIH3T3 cell line using a commercially available plasmid pZsGreen1-C1 from Takara Bio. This GFP expressing plasmid was used as a control since it is designed for in vitro transfection studies as a control plasmid. Lipofectamine 2000, purchased from ThermoFisher Scientific, was used as a positive

transfection reagent control. NIH3T3 cells were seeded on a 24 well plate at 15,000 cells/well for treatment wells, and 30,000 cells/well for positive control wells and incubated at 37 ℃ overnight to allow the cells to attach. The pZsGreen1-C1 plasmid was mixed with lipofectamine reagent according to manufacturer recommendations with 0.5 µg of DNA per well. G5-PEG(3.4K) was mixed with plasmid using batch production method at a 20:1 weight ratio with the same DNA treatment per well. Transfection was done in serum free DMEM for 6 hours at 37 ℃, then an equal volume of serum containing DMEM was added to each well. The cells were then incubated overnight, then media was replaced, and the wells were imaged using a Zeiss Apotome 2 fluorescent microscope. Transfection was monitored from 24-72 hours.

3. RESULTS AND DISCUSSION

3.1. DENDRIMER CONJUGATION

The HNMR Spectrum of Dendrimer conjugates is shown below in Figure 3.1. For PEGylated dendrimer, the spectrum confirms conjugation by the presence of a peak at 3.6 ppm corresponding to methylene protons in the repeating unit of PEG, and G5 dendrimer peaks between 2.3 and 3.3 ppm which arise due to methylene protons of branching units within the dendrimer (Yang, Lopina, DiPersio, & Schmidt, 2008). Integration of the proton peaks corresponding to PEG and G5 dendrimer indicate that an average of 14.7 PEG chains are conjugated to each dendrimer, which confirms the desired conjugation was obtained based on the feeding ratio of PEG to G5 dendrimer. PBA functionalized dendrimer HNMR spectrum shows G5 dendrimer peaks from 2-3.5 ppm and PBA peak at 7.5 which is due to protons on the benzene ring of PBA. Integration of peaks indicate an average of 45 PBA molecules are attached to one G5.

3.2. PLASMID DNA PURIFICATION

DNA purity plays a crucial role in nanocomplex formation due to the complexes being formed through charge interactions. Plasmid purification requires many steps and exposure to multiple lysis solutions which can result in irreversible denaturation of DNA. Plasmid purity was measured by taking the absorbance ratio at 260 and 280 nm respectively for each batch. Absorbance ratios in the range of 1.7-1.9 were used for complex preparation to eliminate the effects of impurities on inhibition of nanocomplex formation.
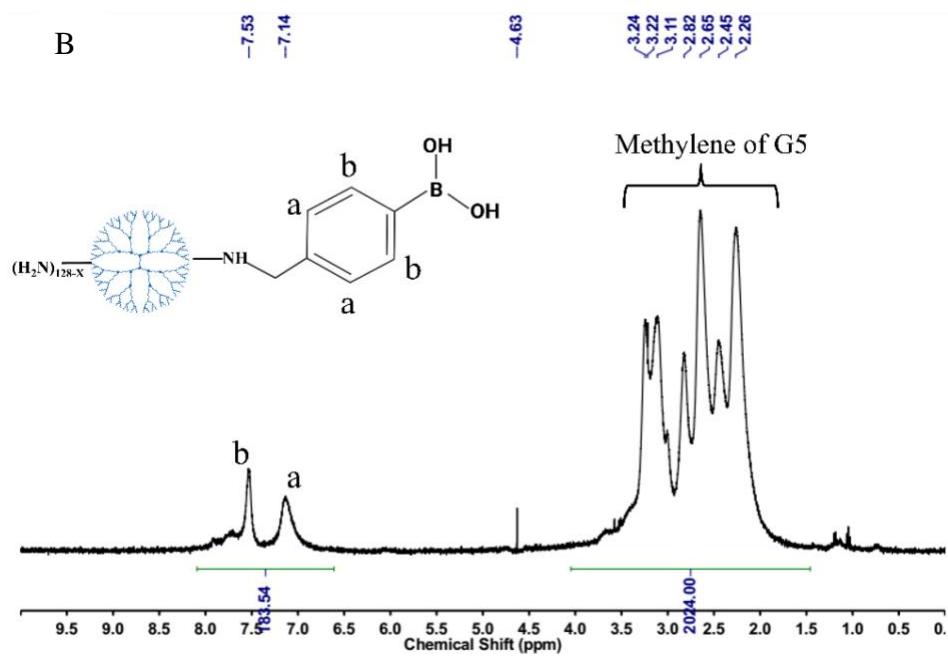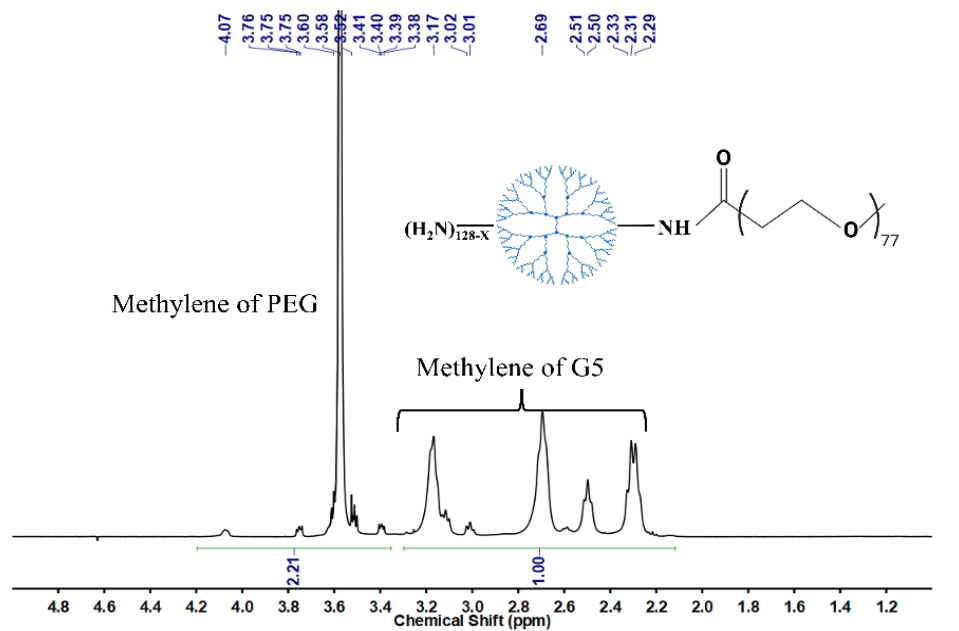
Figure 3.1. H NMR Spectrum of (A) G5-PEG(3.4K) and (B) G5-PBA

Gel retardation assay was conducted to verify the size of the plasmid, and the results can be seen below in Figure 3.2. A 0.8% agarose gel containing ethidium bromide (0.5 µg/mL) was made and allowed to harden at room temperature. DNA samples were loaded along with a DNA ladder to measure the size and subjected to electrophoresis at 100 V for 40 minutes. Gel images for two separate batches of purified DNA are shown below, with absorbance ratios of 1.9 and 1.79, respectively. The DNA ladder shows 3 bright reference bands for size reference at 6000, 3000, and 1000 base pairs, and pcDNA3-EGFP plasmid has a size of 6159 base pairs which corresponds closely to the 6000 base pair band confirming that the purified DNA contains the plasmid of interest.
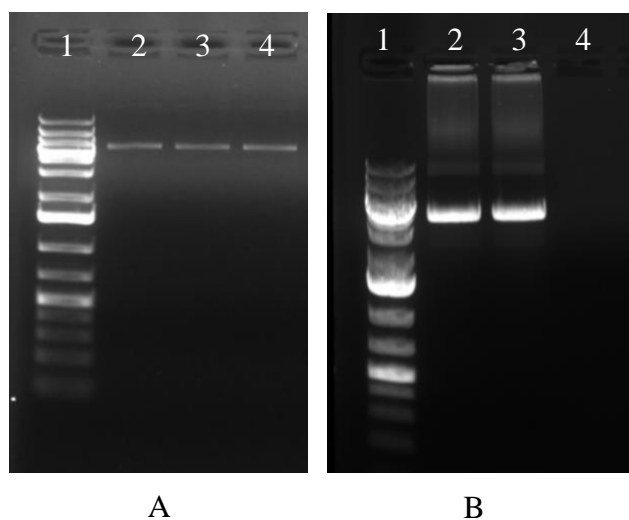
Figure 3.2. Gel Electrophoresis Images of Purified Plasmid DNA (A) Batch 1, Lane 1: DNA Ladder, Lanes 2-4: Purified Plasmid DNA (B) Batch 2, Lane 1: DNA Ladder, Lanes 2-3: Purified Plasmid DNA

3.3. MULTI-INLET VORTEX MIXER FLUID DYNAMICS

The two most important design parameters for scaling of the MIVM are Reynolds number and residence time. Since there is no external agitation mechanism to promote mixing, turbulent flow conditions in the chamber are required to promote mixing. Characterizing Reynolds Number in the chamber allows a design basis for scaling since it is a dimensionless group. The overall Reynolds Number of the mixing system is expressed at the sum of total Re's of individual streams as shown in Equation (1) below (Chow, Sun, & Chow, 2014).

$$Re = \frac{inertial\ forces}{viscous\ forces} = \sum_{1}^{i} Re_i = \sum_{1}^{i} \frac{\rho_i v_i D}{\mu_i} = \frac{\rho D}{\mu_i} \sum_{1}^{i} v_i \tag{1}$$
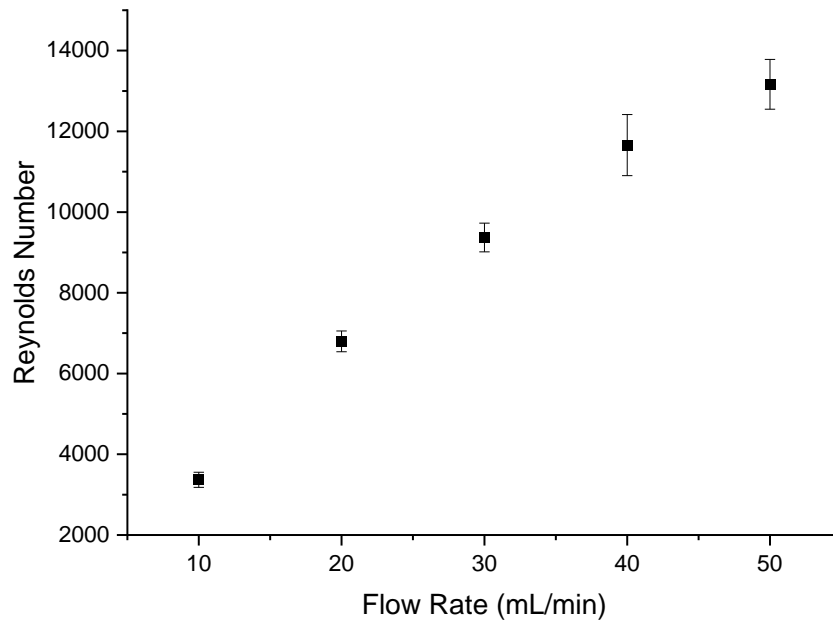
Figure 3.3. Reynolds Number in 3D Printed MIVM at Various Pump Flow Rates

The choice of the definition of the Reynolds number as a linear combination of the stream velocities represents the mixing performance of the MIVM over a relatively wide range of inlet conditions (Y. Liu et al., 2008). The diameter of the chamber was used rather than channel diameter since mixing takes place in the chamber. The inlet velocity of each stream was determined from measured volumetric flow rates and MIVM dimensions. Turbulent conditions were treated the same for fluid flow in pipes which occurs at Reynolds number above 4000. As seen in Figure 3.3. above, turbulent conditions were met except at the lowest flow rate tested which indicates a good mixing regime inside the mixing chamber to enhance contact between all inlet streams. Although higher Reynolds number can lead to larger turbulent conditions, the residence time in the mixing chamber will decrease as the inlet flow rates increase. The residence time at different flow rates can be seen in Figure 3.4. below.
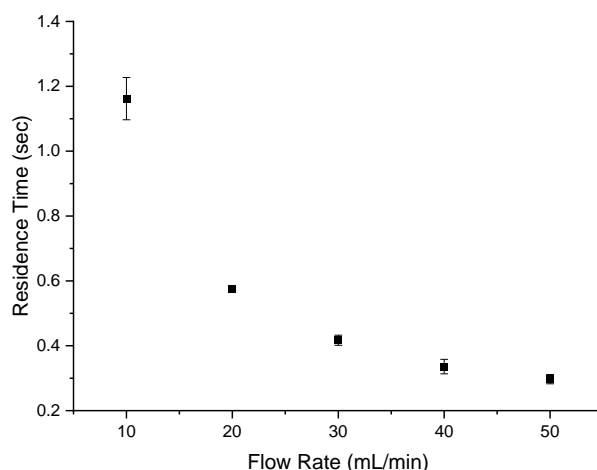
Figure 3.4. Residence Time Distribution in 3D Printed MIVM

The MIVM design yields very low residence times of less than 1 second under turbulent flow conditions. This is in part due to the high flow rate operation, and continuous flow design where material exits immediately. It is assumed that the MIVM mixing chamber behaves as an ideal reactor, and that residence time distributions are negligible and stagnant zones are not present. This agrees with numerical simulations that have shown at Reynolds number above 1600 all of the mixing is completed in the main mixing chamber, but with low Reynolds number, reaction can still take place in the outlet tube (Y. Liu et al., 2008).

3.4. NANOCOMPLEXATION RESULTS

Gel electrophoresis was performed to identify a suitable ratio for dendrimer-plasmid nanocomplexes. G5-PEG(3.4K) was complexed with pcDNA3-EGFP plasmid at various weight ratios. To estimate the amount of free plasmid not complexed with dendrimer, three plasmid controls were used. The controls as identified as plasmid percentages, represent the percentage of plasmid loaded into the nanocomplexes. This control method allows for an estimation of how much free plasmid is not complexed with dendrimers at various weight ratios. The intensity of the bands for nanocomplexes is compared to the controls to identify a suitable ratio for use. According to Figure 3.5.A shown below, a weight ratio of 10 or higher is sufficient to complex most of the plasmid. Although a higher weight ratio can complex all of the plasmid, a lower amount of dendrimer is desired to reduce potential toxicity of nanocomplexes.
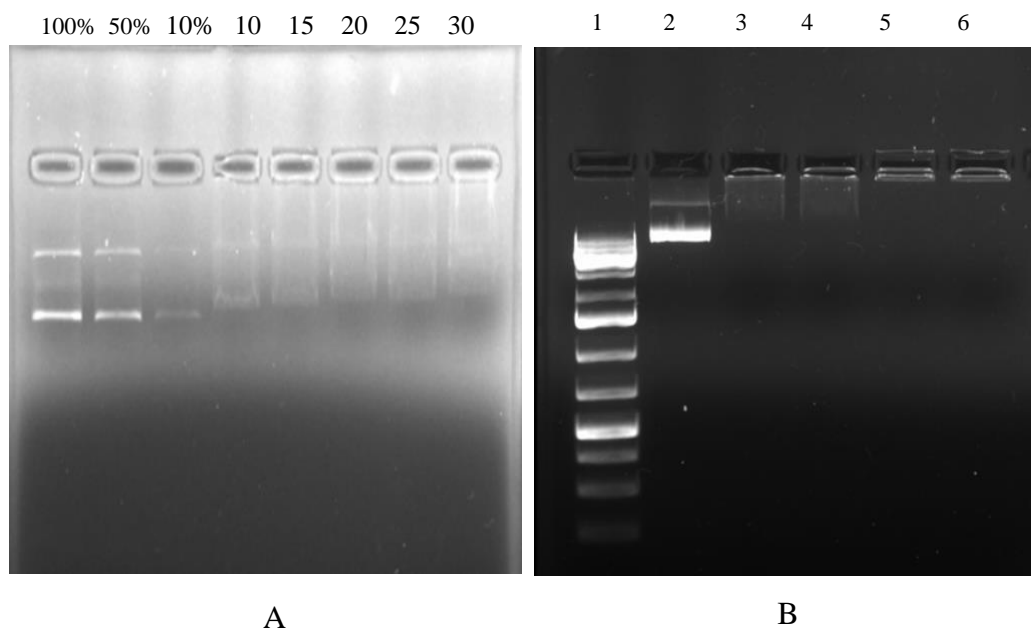
Figure 3.5. Gel Retardation Assay, (A) G5-PEG(3.4K)-pcDNA3-EGFP Nanocomplexes Produced at Weight Ratios of 10, 15, 20, 25, and 30 with 3 Free Plasmid Controls of 100%, 50%, and 10%. (B) G5-PEG(3.4K)-pcDNA3-EGFP Nanocomplexes Produced by MIVM. Lane 1: DNA Ladder, Lane 2: DNA Control, Lanes 3-4: DNA Nanocomplexes Produced in Water, Lanes 5-6 DNA Nanocomplexes Produced in PBS

As used in previous studies (He et al., 2017), a weight ratio of 20:1 was used for plasmid nanocomplexes. Figure 3.5.B shows plasmid nanocomplexes produced in the MIVM in both water and PBS, and the immobility confirms the full complexation of plasmid as compared to the control. Protein nanocomplex formation was verified using FRET assay. The results can be seen in Figure 3.6. below, comparing fluorescence intensity for free protein, free dendrimer, and the protein nanocomplex. A change in the fluorescence intensity is an indication whether complexation took place.
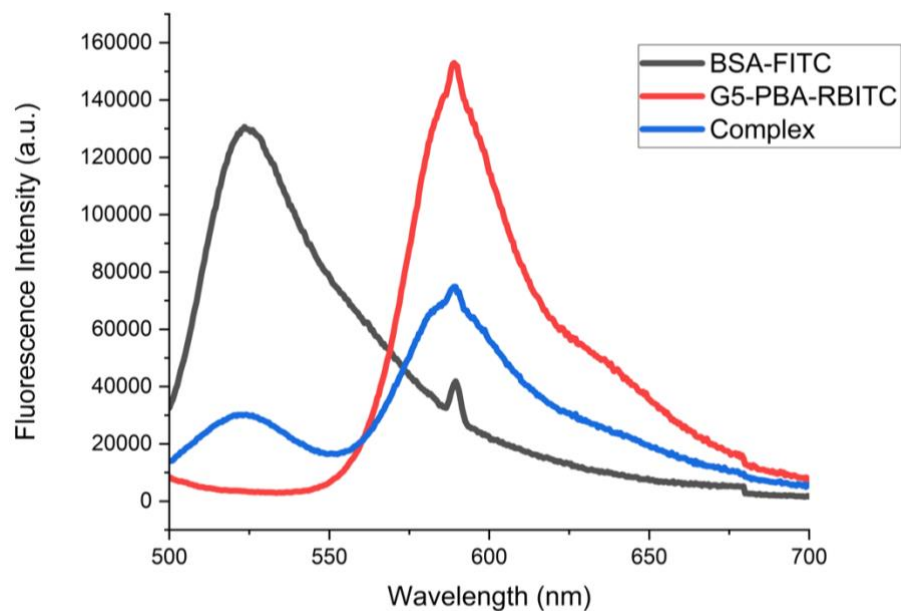
Figure 3.6. Characterization of Protein Nanocomplex by FRET

FRET assay is widely used to study protein-protein interactions and ligand-receptor bindings. The assay works by monitoring energy transfer between two light sensitive molecules. When two molecules are within a short distance to each other, energy transfer can occur. The degree of energy transfer is inversely proportional to the sixth power of the distance between the donor and acceptor, making FRET very senstitive to small changes in distance. The emission wavelength of FITC overlaps with the excitation of RBITC which when the two molecules are close enough together through complex binding, energy transfer occurs. As seen in Figure 3.6. above, the reduction in fluorescence intensity of BSA-FITC and G5-PBA-RBITC individual peaks to that of the complex confirms that a nanocomplex forms between dendrimer and protein.

3.5. BATCH AND CONTINUOUS SIZE DISTRIBUTIONS

Size distribution is an important measure of nanocomplex formation since it is desired to have consistent size of complexes produced. One of the significant drawbacks in batch production of nanocomplexes is inconsistent size distributions between batches, and multiple size populations within a sample. Multiple nanocomplex size populations within a batch may reduce the stability of complexes. As seen in Figure 3.7. below in batch production of DNA and protein nanocomplexes there is poor reproducibility in size distributions from batch to batch. This is due to inconsistent mixing conditions in the vortexing process which is not reproducible or scalable. Both DNA and protein loaded nanocomplex size distributions were measured at various inlet flow rates in the MIVM. Figure 3.8. below shows the size distribution of DNA loaded nanocomplexes produced at various flow rates.
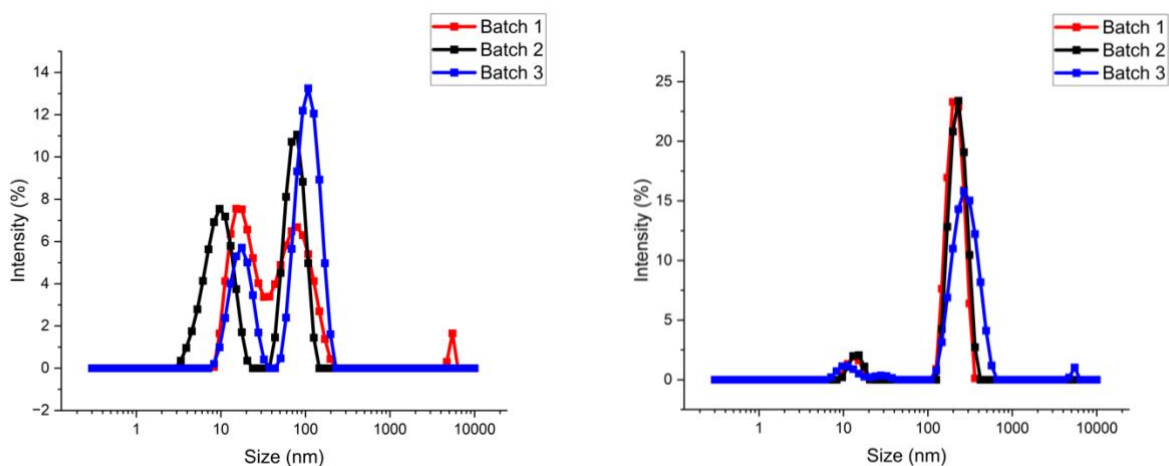
Figure 3.7. Size Distribution of (A) G5-PEG(3.4K)-pcDNA3-EGFP Nanocomplexes and (B) G5-PBA-BSA Nanocomplexes Produced by Batch Production Method
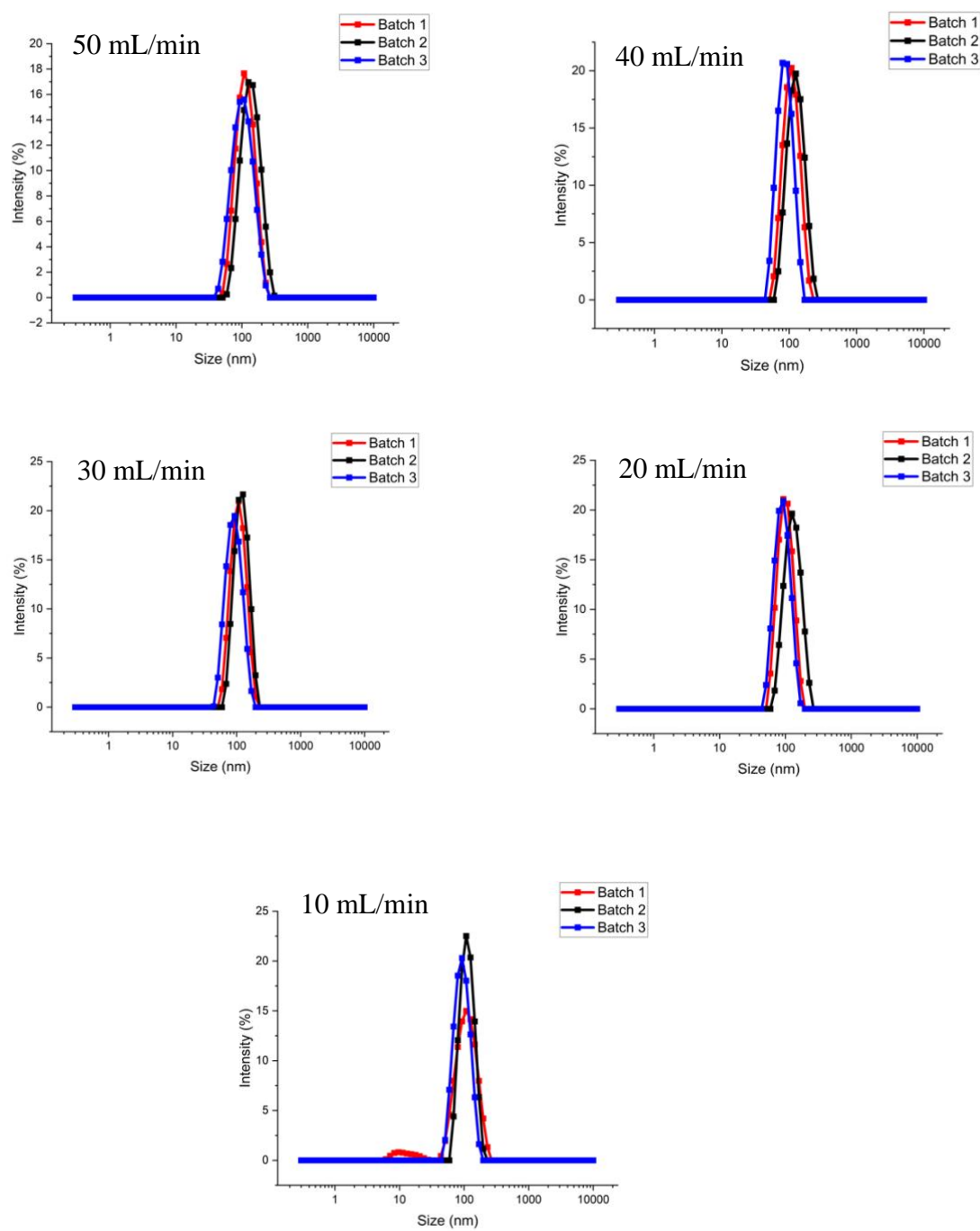
Figure 3.8. Size Distribution of G5-PEG(3.4K)-pcDNA3-EGFP Nanocomplexes
Produced by MIVM at Various Flow Rates Measured by Dynamic Light Scattering

As seen in Table 3.1 below, there is no significant change in mean nanocomplex size at various flow rates for DNA nanocomplexes. However, a decrease in polydispersity index (PDI) is observed as the inlet flow rate increases, indicating that higher turbulence and lower residence time yields a tighter size distribution.

Table 3.1. Mean Size of DNA and Protein Loaded Nanocomplexes Produced by MIVM at Various Flow Rates for 3 Separate Batches

	DNA Nanocomplexes		Protein Nanocomplexes	
Flow Rate (mL/min)	Size (nm)	PDI	Size (nm)	PDI
10	99.8 +/- 14.08	0.3459	184.5 +/- 10.73	0.4244
20	101.1 +/- 15.98	0.3035	215.1 +/- 27.97	0.3271
30	100.2 +/- 15.97	0.3016	190.7 +/- 22.39	0.3629
40	100.4 +/- 14.16	0.2636	180.3 +/- 18.34	0.2875
50	98.52 +/- 14.60	0.2569	171.9 +/- 12.79	0.3001

For protein nanocomplexes, there is a reduction in mean size as flow rate increases, and PDI is generally decreasing as well. The mean size at 10 mL/min does not follow the size reduction trend, and this is likely due to the flow regime being in a laminar-turbulent transition regime due to the lower Reynolds number. Higher flow rates for protein complex formation give more consistent size distributions across multiple batches as compared to lower flow rates. Figure 3.9. shows the size distribution of protein loaded nanocomplexes produced by MIVM at various flow rates.
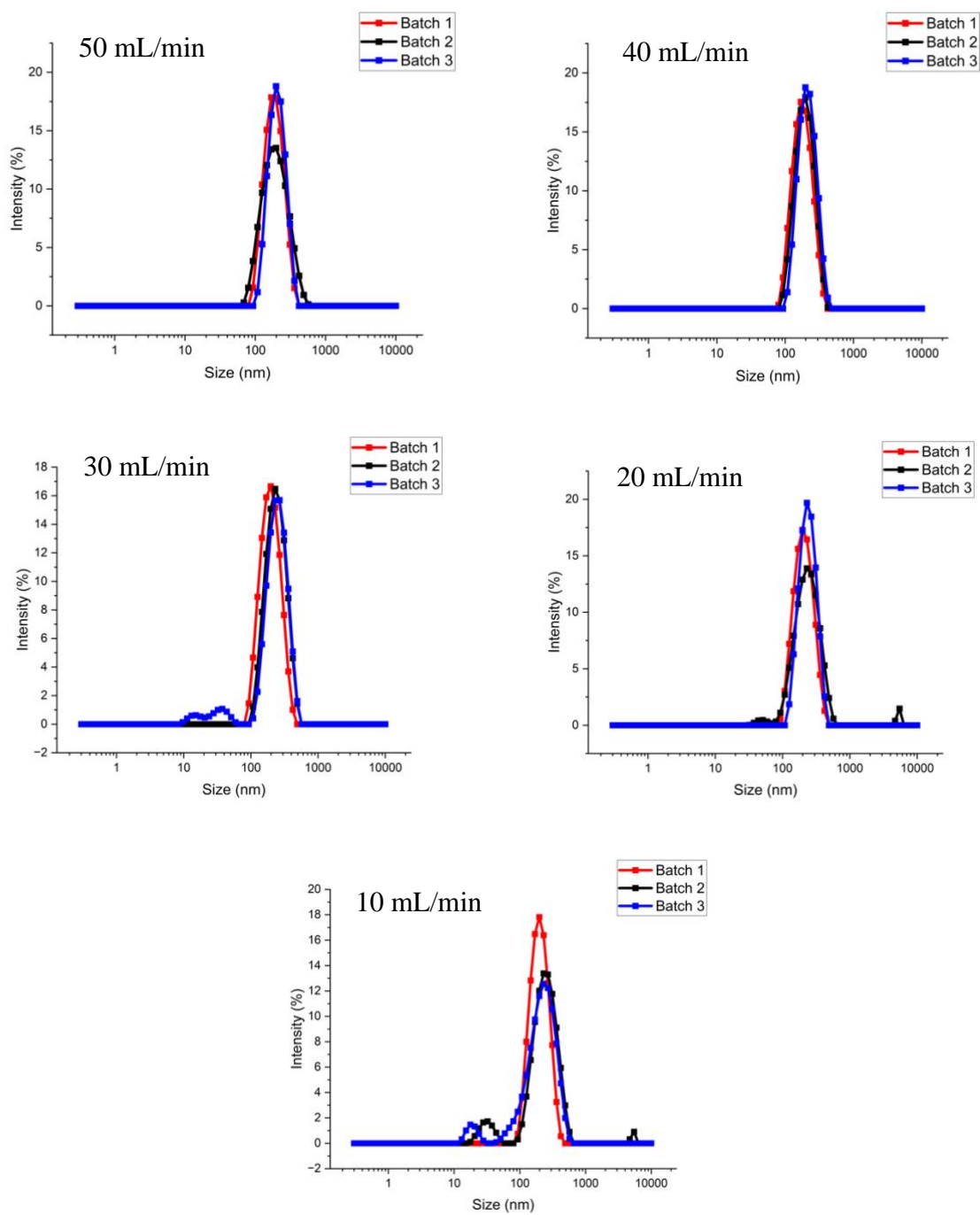
Figure 3.9. Size Distribution of G5-PBA-BSA Nanocomplexes Produced by MIVM at Various Flow Rates Measured by Dynamic Light Scattering

The zeta potential of nanocomplexes was measured for complexes produced by the MIVM at 50 mL/min. Only one flow rate was chosen since the zeta potential is more dependent on the weight ratio and the solvent used rather than the flow rate of the MIVM. The zeta potential for DNA and Protein nanocomplexes produced in water were 22.16 +/- 1.12 mV and 24.53 +/- 1.08 mV, respectively. When nanocomplexes were produced in PBS, the zeta potential was 1.087 +/- 0.4568 mV and 1.752+/- 0.9591 mV for DNA and Protein nanocomplexes, respectively. Nanocomplexes produced in PBS also showed a difference in mean size and polydispersity. As seen in Figure 3.10. below, the size increase in DNA nanocomplexes is only around 20 nm, however for protein nanocomplexes the size increases over 200 nm when produced in PBS.
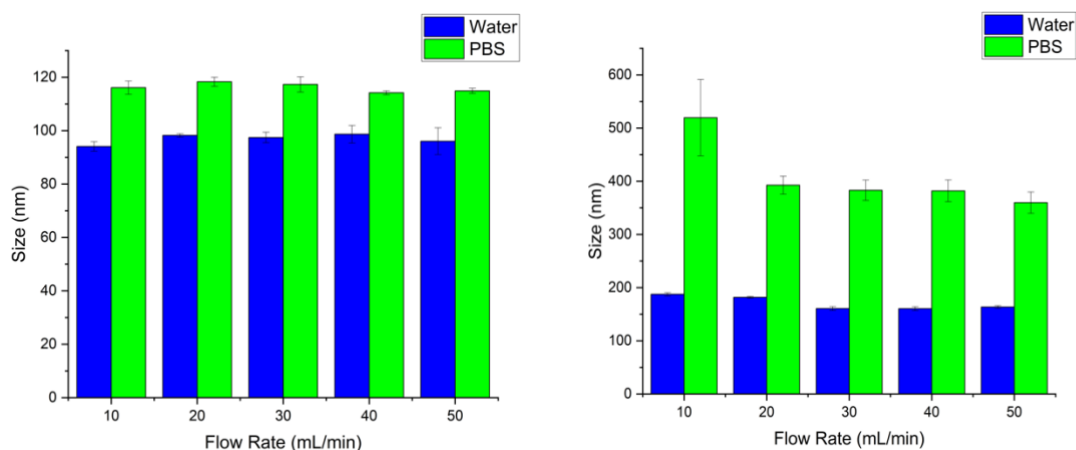
Figure 3.10. Mean Size of (A) DNA Nanocomplexes and (B) Protein Nanocomplexes Produced in Water and PBS

The increase in size when using PBS is likely due to the salts present in solution. Since the nanocomplexes are formed on a charge interaction, ions present in PBS can potentially bind to the dendrimer surface causing larger particles to form. For G5-PEG(3.4K) used in DNA nanocomplexes, the PEG chain does not add any positive charge to the surface, it only reduces the number of amines present which explains why there is not a substantial increase in mean size of complexes produced in PBS. As shown previously all DNA is complexed with dendrimer when made in PBS. However, for G5-PBA, the dendrimer surface charge is enhanced to increase protein binding, which increases the potential for ions present in solution to bind to the dendrimer. This is likely why there is a large increase in particle size of protein nanocomplexes. Table 3.2 below compares the polydispersity index between the complexes produced in both water and PBS. The size distribution of nanocomplexes shows a broad increase in protein nanocomplexes at lower flow rates but they become relatively equal at higher flow rates when comparing water and PBS as solvents, which is also reflected in the mean size of complexes. DNA nanocomplexes do not show much difference in the size distribution regardless of water or PBS being used. The stability of both DNA and Protein loaded nanocomplexes was monitored by measuring the nanocomplex size under different storage conditions. Stability tests were done on nanocomplexes produced at 50 mL/min, and aliquots were stored at room temperature for up to 1 week. Additionally, aliquots were frozen in liquid nitrogen and either allowed to thaw or were lyophilized and resuspended in water. Size distributions from stability tests can be seen below in Figure 3.11.

Table 3.2. Polydispersity Index of DNA and Protein Nanocomplexes Produced in Water and PBS at Various MIVM Flow Rates

Flow Rate (mL/min)	DNA Nanocomplexes		Protein Nanocomplexes	
	PDI (Water)	PDI (PBS)	PDI (Water)	PDI (PBS)
10	0.3021	0.3926	0.3534	0.5305
20	0.3025	0.3242	0.2313	0.3239
30	0.3391	0.3061	0.2758	0.2935
40	0.2577	0.2698	0.2887	0.3082
50	0.2708	0.3256	0.2474	0.2539
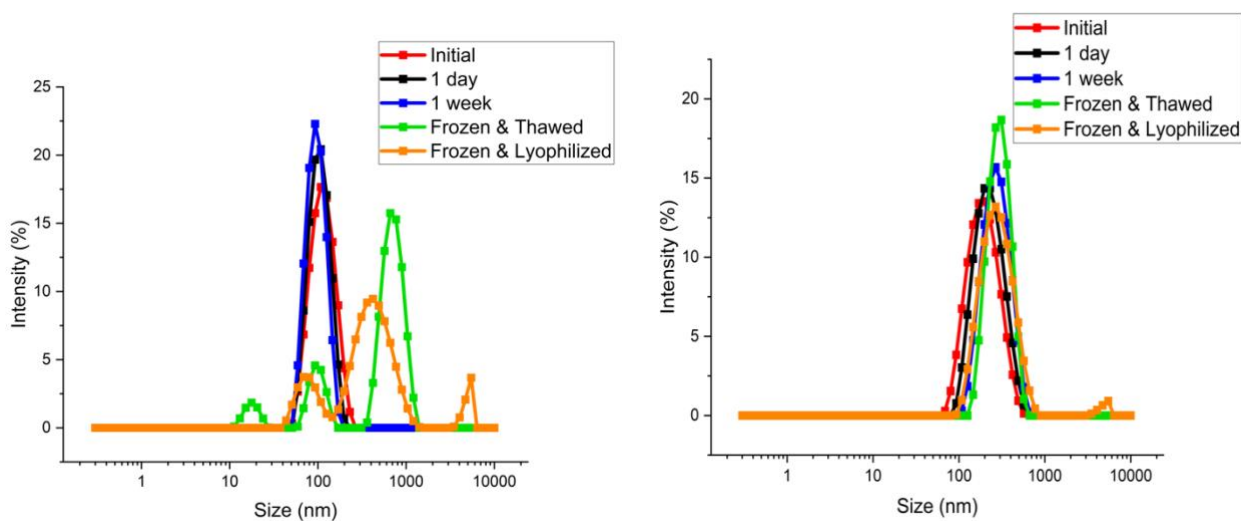
Figure 3.11. Size Distribution of (A) DNA Nanocomplexes and (B) Protein Nanocomplexes Under Different Storage Conditions

DNA loaded nanocomplexes remained stable at room temperature for at least 1 week. Extending past a 1-week period, the solution shows small precipitation which is

likely degradation of the nanocomplexes. Freezing DNA nanocomplexes in liquid nitrogen causes the nanocomplexes to aggregate together to larger sizes regardless of if they are subsequently thawed or lyophilized and resuspended in water. To resolve this issue, a cryoprotectant is likely needed to help stabilize the nanocomplexes during the freezing process.

Protein nanocomplexes showed a slight increase in size after 1 day at room temperature, and further increase after 1 week. Unlike DNA nanocomplexes, freezing protein nanocomplexes in liquid nitrogen showed a slight increase in the size distribution, but the increase was not as significant as DNA nanocomplexes, meaning freezing the protein nanocomplexes may be suitable for long-term storage.

3.6. MAMMILIAN CELL CYTOTOXICITY RESULTS

As shown in Figure 3.12., G5-PEG shows no toxicity in NIH3T3 cells over a 24-hour period. Over the same time period, G5-PBA begins to induce a cytotoxic response in NIH3T3 cells above a concentration of 80 µg/mL. While G5-PBA begins to show cytotoxicity at this concentration, optimal transduction conditions for cytosolic protein delivery is at a much lower dendrimer concentration < 10 µg/mL (C. Liu et al., 2019). Therefore, the observed toxicity is not limiting to protein delivery applications. Although both conjugated dendrimers do not show appreciable toxicity for in vitro application, these results can't gurantee that the same toxicity trends will be seen in other cell lines such as macrophages, HUVEC, and various types of cancer cells.
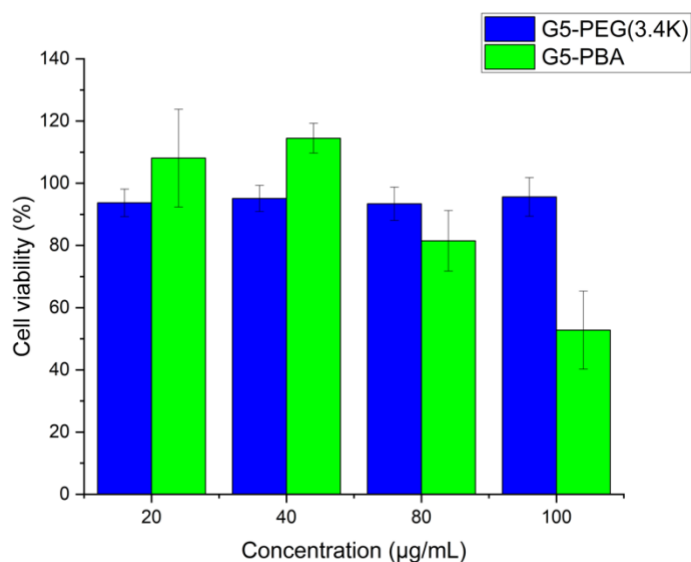
Figure 3.12. Cytotoxicity of Functionalized Dendrimers in NIH3T3 Cells Over a 24- hour Period

3.7. GENE TRANSFECTION RESULTS

After a 24-hour incubation post-transfection, the cells treated with lipofectamine reagent showed positive GFP expression, however the cells treated with the dendrimer-plasmid nanocomplexes showed very little to no GFP expression. There was no GFP expression in the cells treated with dendrimer nanocomplexes. Toxicity was observed after 48 hours in the cells treated with lipofectamine. It is shown below in Figure 3.13. that G5-PEG(3.4K) is easily taken up by the cells, however there is no release of the plasmid payload due to the absence of GFP expression even after 72 hours. This is likely due to the strong charge interaction between the dendrimer and plasmid and further studies are needed to investigate why the payload does not release from the dendrimer.

A

B

C
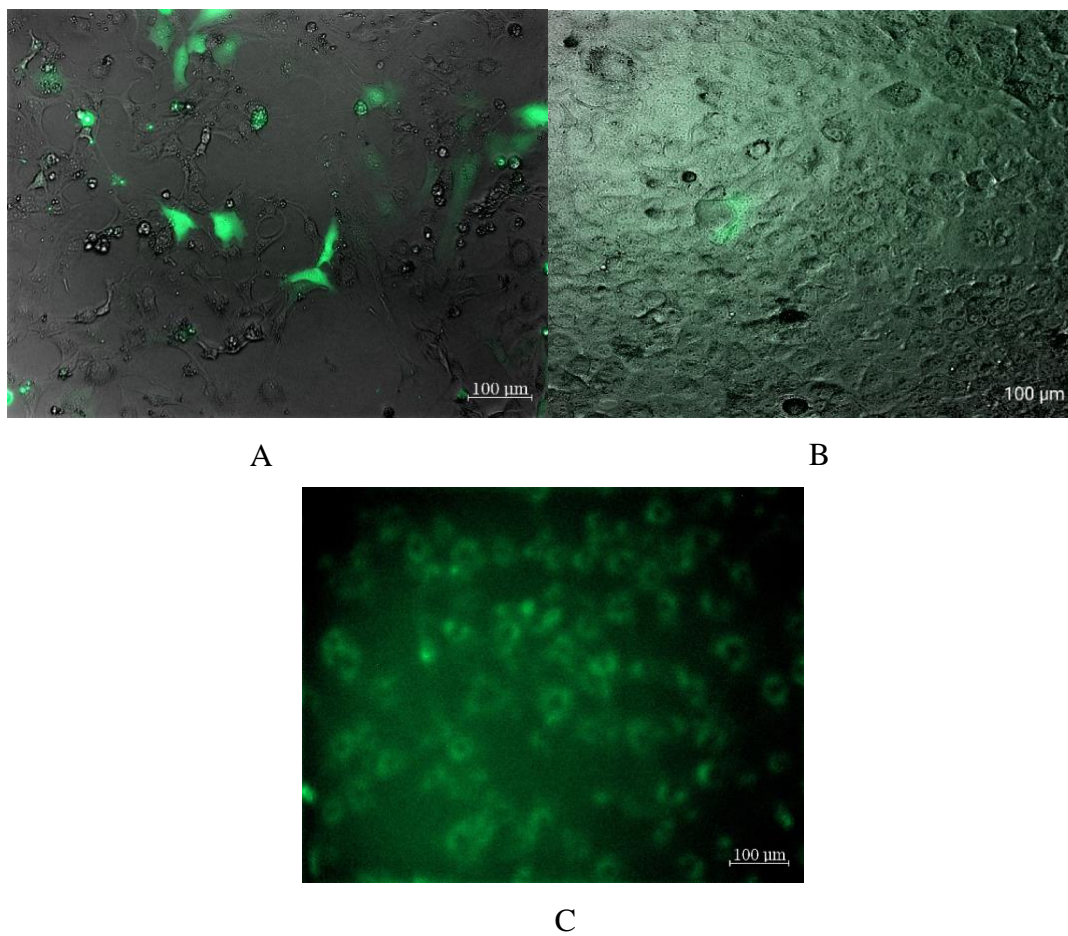
Figure 3.13. Fluorescent Microscope Images of (A) Lipofectamine + pZsGreen1-C1 Positive Control and (B) G5-PEG(3.4K)-pZsGreen1-C1 Nanocomplex after 24 hours and (C) FITC-labeled G5-PEG(3.4K) Internalized in the Cells

4. CONCLUSION

4.1. BENEFITS OF MULTI-INLET VORTEX MIXER PLATFORM

The MIVM as a mixing platform for continuous production of dendrimer based nanocomplexes has been shown. Operation of the MIVM at high Reynolds number yields consistent size distributions of nanocomplexes across multiple batches allowing for a scalable approach for manufacturing. In this study the specific nanocomplexes produced appeared to not be critically affected by flow rate for the MIVM. Among the two solvents tested, production in water tended to be a more suitable option than PBS, which can be observed by the smaller particle size, and lower PDI for both DNA and protein loaded nanocomplexes. 3D printing the MIVM allows for easy manipulation of the geometry and ability to print multiple devices at once for testing. Using a clear resin to make the MIVM provides the benefit of visually monitoring fluid flow in the MIVM. This is important to ensure that there is no entrapment of air bubbles, leaking, or backflow into one of the inlet streams. Overall, operation of the MIVM provides a wide range of benefits as a mixing platform for continuous production.

4.2. NEXT STEPS AND FUTURE WORK

The project can continue in many routes. For MIVM production, since there was no major effect of flow rate on size distribution and stability of both DNA and protein nanocomplexes, different feeding ratios can be tested to see if the optimal weight ratio changes when using the MIVM system. Similarly, synthesis in different solvents can be tested. As mentioned, when using a buffer as the solvent, salts present in the solution can

inhibit the degree of complexation since the nanocomplexes are formed from charged interactions. Nanocomplexes produced in PBS, or cell culture media may not yield the same size distribution and stability as those produced in water due to the compounds present in the solvent. The biological application of formulations produced through MIVM should be investigated to validate that manufacturing nanocomplexes through MIVM does not sacrifice functionality as compared to the batch method. Application studies include gene transfection, and cytosolic protein delivery across multiple cell lines. Similarly, evaluating the MIVM as a platform for loading various payloads such as mRNA, siRNA, and small drugs into dendrimers should be evaluated.

BIBLIOGRAPHY

Banting, F. G., Best, C. H., Collip, J. B., Campbell, W. R., & Fletcher, A. A. (1922). Pancreatic Extracts in the Treatment of Diabetes Mellitus. *Canadian Medical Association journal, 12*(3), 141-146.

Berényi, S., Mihaly, J., Wacha, A. F., Toke, O., & Bóta, A. (2014). A mechanistic view of lipid membrane disrupting effect of PAMAM dendrimers. *Colloids and surfaces. B, Biointerfaces, 118C*, 164-171. doi:10.1016/j.colsurfb.2014.03.048

Chow, S. F., Sun, C. C., & Chow, A. H. L. (2014). Assessment of the relative performance of a confined impinging jets mixer and a multi-inlet vortex mixer for curcumin nanoparticle production. *European Journal of Pharmaceutics and Biopharmaceutics, 88*(2), 462-471. doi:https://doi.org/10.1016/j.ejpb.2014.07.004

He, H., Lancina, M. G., 3rd, Wang, J., Korzun, W. J., Yang, H., & Ghosh, S. (2017). Bolstering cholesteryl ester hydrolysis in liver: A hepatocyte-targeting gene delivery strategy for potential alleviation of atherosclerosis. *Biomaterials, 130*, 1-13. doi:10.1016/j.biomaterials.2017.03.024

Johnson, B. K., & Prud'homme, R. K. (2003). Chemical processing and micromixing in confined impinging jets. *AIChE Journal, 49*(9), 2264-2282. doi:https://doi.org/10.1002/aic.690490905

Leader, B., Baca, Q. J., & Golan, D. E. (2008). Protein therapeutics: a summary and pharmacological classification. *Nature Reviews Drug Discovery, 7*(1), 21-39. doi:10.1038/nrd2399

Liu, C., Wan, T., Wang, H., Zhang, S., Ping, Y., & Cheng, Y. (2019). A boronic acid–rich dendrimer with robust and unprecedented efficiency for cytosolic protein delivery and CRISPR-Cas9 gene editing. *Science Advances, 5*(6), eaaw8922. doi:doi:10.1126/sciadv.aaw8922

Liu, Y., Cheng, C., Liu, Y., Prud'homme, R. K., & Fox, R. O. (2008). Mixing in a multi-inlet vortex mixer (MIVM) for flash nano-precipitation. *Chemical Engineering Science, 63*(11), 2829-2842. doi:https://doi.org/10.1016/j.ces.2007.10.020

Mudshinge, S. R., Deore, A. B., Patil, S., & Bhalgat, C. M. (2011). Nanoparticles: Emerging carriers for drug delivery. *Saudi Pharmaceutical Journal, 19*(3), 129-141. doi:https://doi.org/10.1016/j.jsps.2011.04.001

Verma, I. M., & Weitzman, M. D. (2005). GENE THERAPY: Twenty-First Century Medicine. *Annual Review of Biochemistry, 74*(1), 711-738. doi:10.1146/annurev.biochem.74.050304.091637

Yang, H., Lopina, S. T., DiPersio, L. P., & Schmidt, S. P. (2008). Stealth dendrimers for drug delivery: correlation between PEGylation, cytocompatibility, and drug payload. *Journal of Materials Science: Materials in Medicine, 19*(5), 1991-1997. doi:10.1007/s10856-007-3278-0

Yuan, Q., Yeudall, W. A., & Yang, H. (2010). PEGylated Polyamidoamine Dendrimers with Bis-Aryl Hydrazone Linkages for Enhanced Gene Delivery. *Biomacromolecules, 11*(8), 1940-1947. doi:10.1021/bm100589g

Zhu, Z. (2014). Flash Nanoprecipitation: Prediction and Enhancement of Particle Stability via Drug Structure. *Molecular Pharmaceutics, 11*(3), 776-786. doi:10.1021/mp500025e

VITA

Joseph Timothy Johnston was born and raised in Kansas City, Missouri. He attended Missouri University of Science and Technology where he earned a Bachelor of Science in Chemical Engineering with a Minor in Chemistry in May 2021. During his undergraduate years, he completed internships with Northrop Grumman and ExxonMobil, and undergraduate research under Dr. Sutapa Barua. He stayed at Missouri University of Science and Technology to pursue graduate studies in the chemical engineering department under the supervision of Dr. Hu Yang. He received a graduate certificate in Chemical Process Engineering and his Master of Science in Chemical Engineering in July 2022.